Mathematical Biosciences and Engineering

MBE, 19(1): 169–190.
DOI: 10.3934/mbe.2022009
Received: 30 July 2021
Accepted: 27 September 2021
Published: 09 November 2021

http://www.aimspress.com/journal/MBE

Research article

PVT1 is a prognostic marker associated with immune invasion of bladder urothelial carcinoma

Peiyuan Li[1], Gangjie Qiao[1], Jian Lu[2], Wenbin Ji[1], Chao Gao[1] and Feng Qi[1,*]

[1] Department of General Surgery, Tianjin Medical University General Hospital, No. 154, Anshan Road, Heping District, Tianjin 300052, China.
[2] Department of Gastroenterology, The First Affiliated Hospital of Anhui Medical University, No. 218, Jixi Road, Shushan District, Hefei 230022, China.

* **Correspondence:** Email: qf@medmail.com.cn, qifengtmu2017@163.com.

Abstract: Plasmacytoma variant translocation 1 (PVT1) is involved in multiple signaling pathways and plays an important regulatory role in a variety of malignant tumors. However, its role in the prognosis and immune invasion of bladder urothelial carcinoma (BLCA) remains unclear. This study investigated the expression of PVT1 in tumor tissue and its relationship with immune invasion, and determined its prognostic role in patients with BLCA. Patients were identified from the cancer genome atlas (TCGA). The enrichment pathway and function of PVT1 were explained by gene ontology (GO) term analysis, gene set enrichment analysis (GSEA) and single-sample gene set enrichment analysis (ssGSEA), and the degree of immune cell infiltration was quantified. Kaplan–Meier analysis and Cox regression were used to analyze the correlation between PVT1 and survival rate. PVT1-high BLCA patients had a lower 10-year disease-specific survival (DSS $P < 0.05$) and overall survival (OS $P < 0.05$). Multivariate Cox regression analysis showed that PVT1 (high vs. low) ($P = 0.004$) was an independent prognostic factor. A nomogram was used to predict the effect of PVT1 on the prognosis. PVT1 plays an important role in the progression and prognosis of BLCA and can be used as a medium biomarker to predict survival after cystectomy.

Keywords: PVT1; bioinformatics; biomarker; bladder urothelial carcinoma; immune infiltration

1. Introduction

Bladder cancer is the second most common malignant tumor of the urinary system, causing more

than 165,000 deaths worldwide every year [1]. Despite great advances in understanding the molecular mechanisms and surgical techniques underlying bladder cancer in the past few years, the mortality rate from bladder cancer has not decreased significantly [2]. Bladder urothelial carcinoma (BLCA) is the fifth most common human cancer diagnosis. In 2016, more than 76000 people were diagnosed with carcinoma of the urinary bladder. In addition, 16000 patients are expected to be die from the disease [3]. One main reason is that the exact molecular mechanisms underlying bladder urothelial carcinoma metastasis and progression are still poorly understood. It is very important to find new and reliable biomarkers to reveal the molecular mechanisms of bladder urothelial carcinoma.

Plasmacytoma variant translocation 1 (PVT1) maps at the 8q24.21 chromosomal band [chr8:127, 795, 799–128, 187,101 (GRCh38/hg38)], 55 kb downstream of the MYC gene [4]. PVT1 RNA and MYC protein expression are correlated in primary human tumors, and PVT1 copy number increases together with increased *MYC* copy number in more than 98% of tumors [5]. PVT1 is closely associated with cancer [6–8]. PVT1 is an active oncogene that plays an important role in the pathogenesis of many tumors; PVT1 linear and circular isoforms are consistently expressed in bladder [9], breast [10], cervix [11], colon [12], lung [13], ovarian [14], and prostate [15] cancers. Moreover, high PVT1 expression levels are found in several hematological malignancies such as acute myeloid leukemia (AML) [16,17], acute lymphoblastic leukemia (ALL) [18], and multiple myeloma [19] (MM). Most of the carcinogenic functions of PVT1 are unknown, but some studies have shown that this lncRNA is a powerful inducer of cell proliferation and tumor growth [20–22]. In fact, *PVT1* knockout results in loss of cell proliferation and activity in lung cancer [23] and colon cancer [24], as well as retinoblastoma [25]. The mechanism of the carcinogenic function of PVT1 is multifaceted and still not completely clear; however, it is a strong competitive endogenous RNA (ceRNA) that competes with mRNAs for the combination of miRNAs [26]. In cancer, both lncRNAs and circRNAs can bind to several miRNAs, thereby weakening miRNA-dependent oncogene suppression [27].

In previous studies, we found that PVT1 is also closely associated with bladder cancer. PVT1 is involved in malignant progression and development of bladder carcinomas as a ceRNA [28]. PVT1 might play a critical role in bladder cancer tumorigenesis via miR-218 and VEGFC [29]. However, the role and mechanism of PVT1 in tumor progression and immunity are unclear.

In this study, we used RNA sequencing data from the cancer genome atlas (TCGA) database, combined with bioinformatics and statistical methods, differentially expressed gene (DEG) analysis, gene ontology (GO) term analysis, Kyoto encyclopedia of genes and genomes (KEGG) pathway analysis, gene set enrichment analysis (GSEA), single-sample gene set enrichment analysis (ssGSEA), and Kaplan-Meier survival analysis. The significance of PVT1 in BLCA was analyzed systematically. In addition, we developed a nomogram to predict patient outcomes.

2. Results

2.1. Expression of PVT1 in BLCA

First, pan-cancer analysis of was performed. The UCSC XENA database was selected for analysis, and the results were obtained using the Wilcoxon rank-sum test. PVT1 was significantly expressed in adrenocortical carcinoma (ACC), bladder urothelial carcinoma (BLCA), breast invasive carcinoma (BRCA), cholangiocarcinoma (CHOL), colon adenocarcinoma (COAD), lymphoid neoplasm diffuse large B-cell lymphoma (DLBC), esophageal carcinoma (ESCA), glioblastoma multiforme (GBM),

head and neck squamous cell carcinoma (HNSC), kidney renal clear cell carcinoma (KIRC), kidney renal papillary cell carcinoma (KIRP), acute myeloid leukemia (LAML), brain lower grade glioma (LGG), liver hepatocellular carcinoma (LIHC), lung adenocarcinoma (LUAD), lung squamous cell carcinoma (LUSC), ovarian serous cystadenocarcinoma (OV), pancreatic adenocarcinoma (PAAD), rectum adenocarcinoma (READ), skin cutaneous melanoma (SKCM), stomach adenocarcinoma (STAD), testicular germ cell tumors (TGCT), thyroid carcinoma (THCA), thymoma (THYM) ($P < 0.05$) (Figure 1A). Second, we compared 435 unpaired samples of bladder uroepithelial carcinoma from TCGA combined with the GTEx database, and found that PVT1 was highly expressed in the carcinoma tissue ($P = 0.001$) (Figure 1B). In addition, we compared 433 paired samples of bladder urothelial carcinoma from TCGA database and found that PVT1 was highly expressed in the carcinoma tissue ($P < 0.005$) (Figure 1C).

Receiver operating characteristic (ROC) analysis was used to analyze the differentiation effect of PVT1 between carcinoma and normal tissue in bladder urothelial carcinoma. The area under the curve of PVT1 was 0.816, suggesting that PVT1 had a certain accuracy in predicting tumor and normal outcomes (Figure 1D).

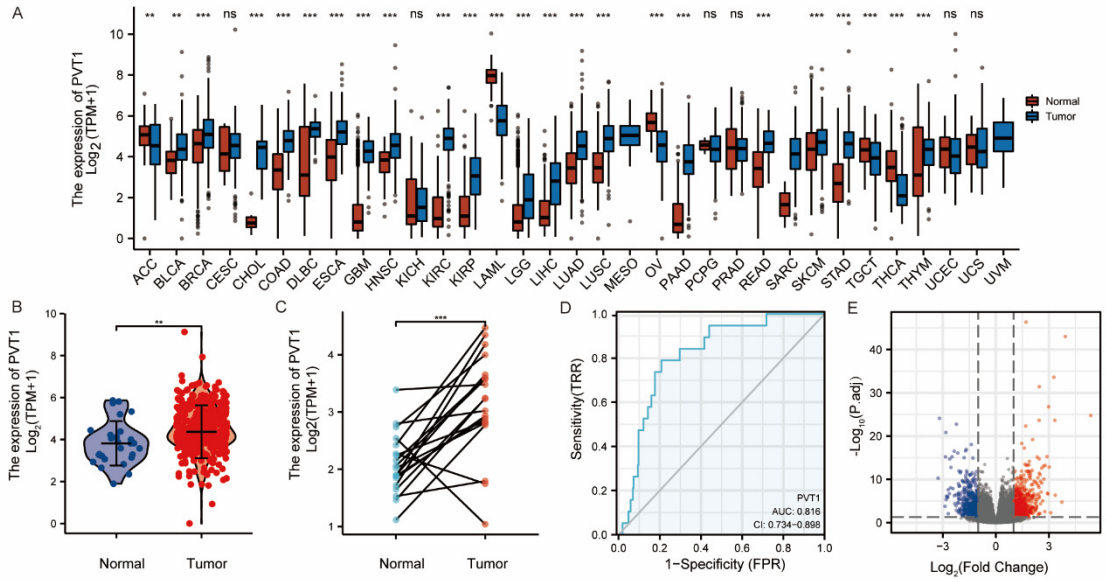

Figure 1. The expression level of PVT1 was different in different malignant tumors and PVT1-related differentially expressed genes. (A) The PVT1 of different cancers in TCGA and GTEx databases compared with normal tissues. (B) Differential expression level of PVT1 in unpaired samples of BLCA. (C) Differential expression level of PVT1 in paired samples of BLCA. (D) A ROC curve established to test the value of PVT1 to identify BLCA tissues. (E) Volcanic map of DEGs.

2.2. Analysis of single gene difference of PVT1 in BLCA

A total of 433 samples from TCGA database were used to analyze the single gene differences in PVT1. There were 635 upregulated genes and 544 downregulated genes (adjusted p-value < 0.05, |Log2-fold change| > 1). The differential genes were represented by a volcano map (Figure 1E). The

string database and Cytoscope were used for protein-protein interaction (PPI) network analysis of differential genes, as well as a score > 10 protein interaction network for single gene co-expression heat map analysis (Figure 2A-D). PVT1 was positively correlated with *KRT6B*, *KRT79*, *KRT5*, *KRT16*, *KRT6C*, *KRT3*, *KRT14*, *KRT13*, *KRT6A*, *KRT74*, *KRT15*, *KRT81*, *PPY*, *QRFPR*, and *GAL* ($P < 0.005$). PVT1 was negatively correlated with *GRM6*, *SST*, *GABBR2*, *XCR1*, *CCKAR*, *HRH3*, *GRM3*, *TAS2R1*, *F2*, *CASR*, *AGTR2*, and *TAC3* ($P < 0.005$).

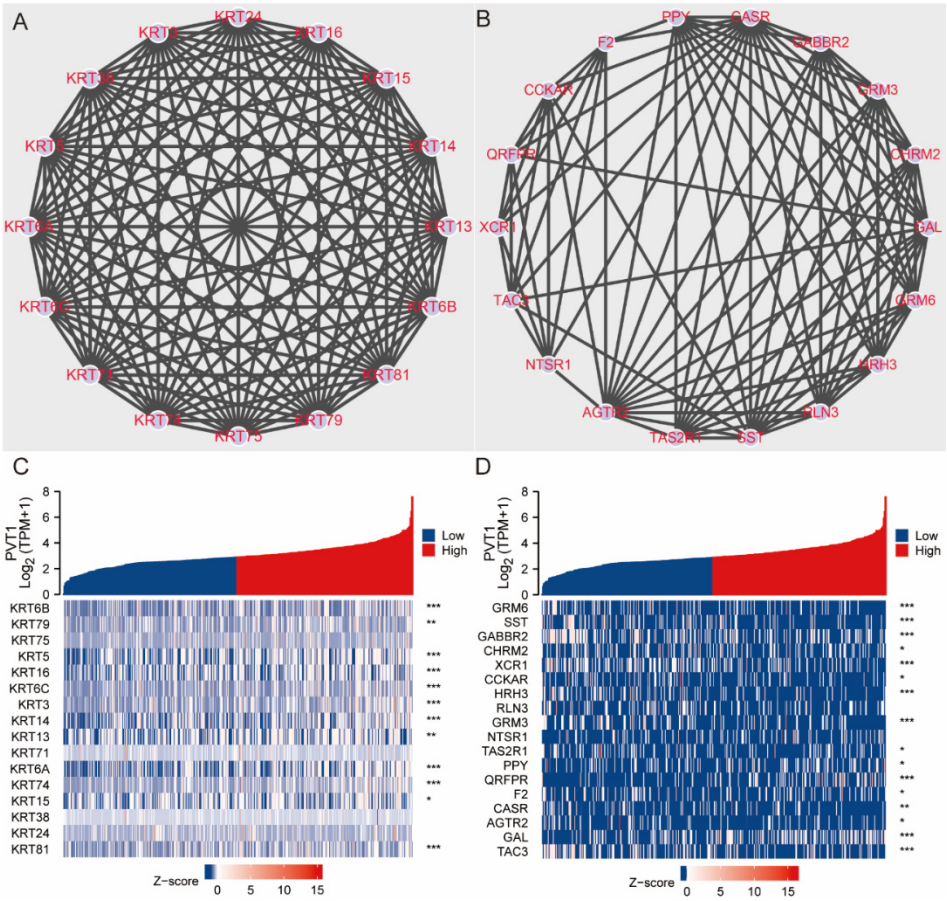

Figure 2. Differential analysis of *PVTI* single gene in BLCA. (A) PPI network map of upregulated genes associated with PVT1. (B) PPI network map of downregulated genes associated with PVT1. (C) Heat map of upregulated genes associated with PVT1. (D) Heat map of downregulated genes associated with PVT1.

2.3. Function enrichment and analysis of PVT1 in BLCA

Functional enrichment analysis of the differentially expressed genes was performed using GO and KEGG (Figure 3A, Table 1). The results showed that PVT1-related genes are involved in many biological processes (BPs), cellular composition (CCs), and molecular functions (MFs), including cornification, intermediate filaments, hormone activity, and receptor ligand activity. KEGG analysis of surface differential genes involved neuroactive ligand-receptor interaction, bile secretion, and metabolism of xenobiotics by cytochrome P450.

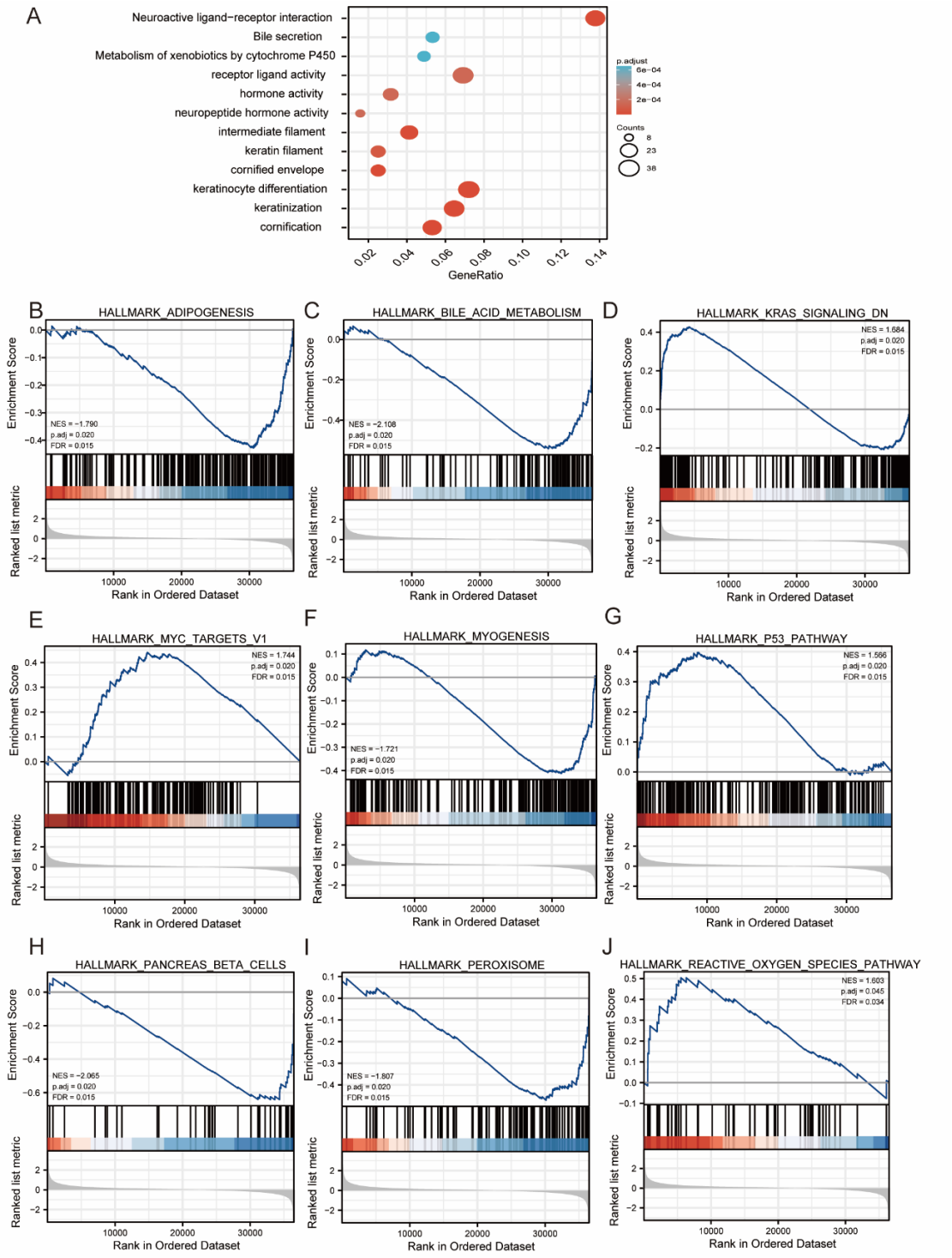

Figure 3. Significantly enriched GO and KEGG annotations of PVT1-related genes in BLCA. (A) The bar chart shows the top three enrichment positions of biological processes associated with PVT1-related genes. (B–J) Enrichment plots from the gene set enrichment analysis (GSEA). BLCA associated with PVT1 had a variety of pathways and biological processes. Several pathways and biological processes significantly enriched in PVT1-related BLCA were demonstrated. NES, normalized enrichment score; p.adj, adjusted P–value; FDR, false discovery rate.

Table 1. Go and KEGG analysis.

ONTOLOGY	ID	Description	GeneRatio	BgRatio	pvalue	p.adjust	qvalue
BP	GO:0070268	cornification	28/527	112/18670	4.42e–19	1.61e–15	1.46e–15
BP	GO:0031424	keratinization	34/527	224/18670	1.00e–15	1.83e–12	1.65e–12
BP	GO:0030216	keratinocyte differentiation	38/527	305/18670	1.48e–14	1.80e–11	1.63e–11
BP	GO:0009913	epidermal cell differentiation	40/527	358/18670	1.14e–13	9.33e–11	8.45e–11
BP	GO:0008544	epidermis development	46/527	464/18670	1.28e–13	9.33e–11	8.45e–11
CC	GO:0001533	cornified envelope	14/558	65/19717	2.91e–09	1.15e–06	1.01e–06
CC	GO:0005882	intermediate filament	23/558	214/19717	4.62e–08	9.13e–06	8.00e–06
CC	GO:0045095	keratin filament	14/558	95/19717	4.48e–07	5.89e–05	5.17e–05
CC	GO:0045111	intermediate filament cytoskeleton	23/558	251/19717	8.24e–07	8.13e–05	7.13e–05
CC	GO:0031225	anchored component of membrane	15/558	170/19717	1.02e–04	0.007	0.007
MF	GO:0005179	hormone activity	16/506	122/17697	3.98e–07	1.39e–04	1.23e-04
MF	GO:0048018	receptor ligand activity	35/506	482/17697	4.69e–07	1.39e–04	1.23e–04
MF	GO:0005184	neuropeptide hormone activity	8/506	28/17697	7.93e–07	1.57e–04	1.39e–04
MF	GO:0030414	peptidase inhibitor activity	18/506	182/17697	5.00e–06	6.72e–04	5.95e–04
MF	GO:0005200	structural constituent of cytoskeleton	13/506	102/17697	6.72e–06	6.72e–04	5.95e–04
KEGG	hsa04080	Neuroactive ligand-receptor interaction	31/225	341/8076	4.35e–09	1.05e–06	9.58e–07
KEGG	hsa04976	Bile secretion	12/225	90/8076	6.56e–06	6.51e–04	5.97e–04
KEGG	hsa00980	Metabolism of xenobiotics by cytochrome P450	11/225	77/8076	8.14e–06	6.51e–04	5.97e–04
KEGG	hsa05204	Chemical carcinogenesis	11/225	82/8076	1.51e–05	7.82e–04	7.16e–04
KEGG	hsa00830	Retinol metabolism	10/225	68/8076	1.63e–05	7.82e–04	7.16e–04

2.4. GSEA identified PVT1-related signaling pathways

To identify PVT1-related signaling pathways in BLCA, GSEA analysis was performed on high and low PVT1 expression datasets. The MSigDB Collection (h.all.v7.2.symbols.gmt [Hallmark])

showed significant differences in enrichment (false discovery rate [FDR] < 0.25, *p*.adjust < 0.05). Selecting significantly enriched signaling pathways, the differential enrichment pathways of PVT1 low and high expression groups included adipocyte development, biosynthesis of bile acids, KRAS signaling (down-regulated), MYC Targets Variant 1, muscle differentiation, p53 pathway, genes specific to pancreatic beta cells, peroxisomes, and the reactive oxygen species pathway (Figures 3B–J).

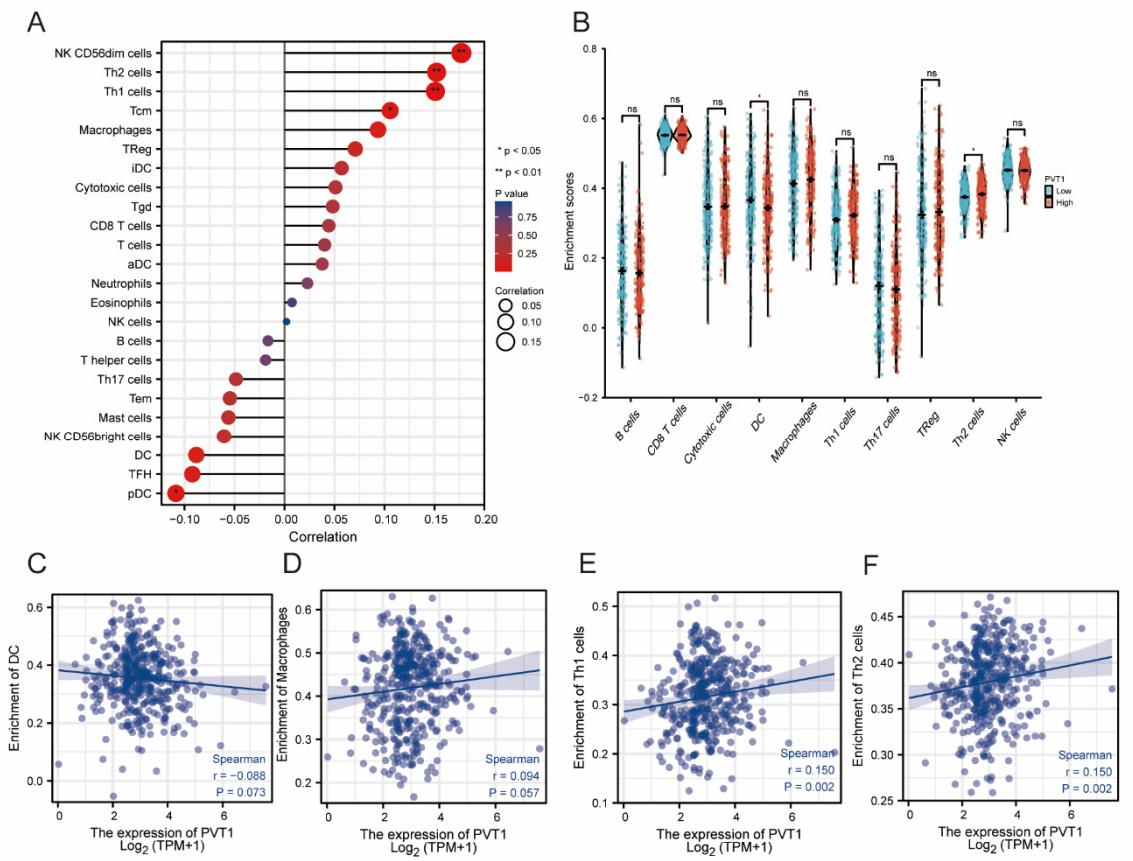

Figure 4. The expression level of PVT1 was associated with immune invasion in the tumor microenvironment. (A) Correlation between the relative abundance of 24 immune cells and PVT1 expression levels. (B) According to the expression of PVT1, the gene set was divided into high and low groups, and the infiltration of immune cells was compared. (C–F) Scatter plots and correlation diagrams showing the difference of Th1 cells and Th2 cells infiltration level between PVT1-high and -low groups.

2.5. Relationship between PVT1 expression and immune infiltration

Spearman correlation was used to analyze the correlation between PVT1 expression levels and ssGSEA quantitative immune cell infiltration levels. The expression of PVT1 was positively correlated with acquired immune cells (Th17 cells, T helper [Th] cells, T central memory cells) ($P < 0.005$), and negatively correlated with pDC ($P < 0.005$) (Figure 4A).

According to the expression level of PVT1, the gene set was divided into two groups. According to the ssGSEA algorithm, the expression levels of PVT1 in DC and Th2 were statistically significant

($P < 0.05$) (Figure 4B). Analysis of PVT1 expression and related immune cells showed that PVT1 was significantly positively correlated with Th1 and Th2 expression ($P < 0.05$) (Figures 4C–F).

2.6. Relationship between PVT1 expression and clinicopathologic variables

To investigate the correlation between PVT1 and clinical indicators, 433 cases of BLCA were collected from TCGA, and the baseline data sheet was completed according to the level of PVT1 expression (Table 2). As shown in Figures 5A–I, among the relationships between PVT1 and clinical characteristics, there was no significant correlation between PVT1 and age, BMI, Smoking status, radiation therapy ($P > 0.05$). In TNM stage, histologic grade, and pathologic stage, except N3 vs. normal, T1 vs. normal, and pathology stage I vs. normal, the comparison of other groups showed that the expression of PVT1 in patients was different from that in normal people ($P < 0.05$). However, the expression level of PVT1 was not significantly different among the different stages of TNM stage, histologic grade, or pathologic stage ($P > 0.05$).

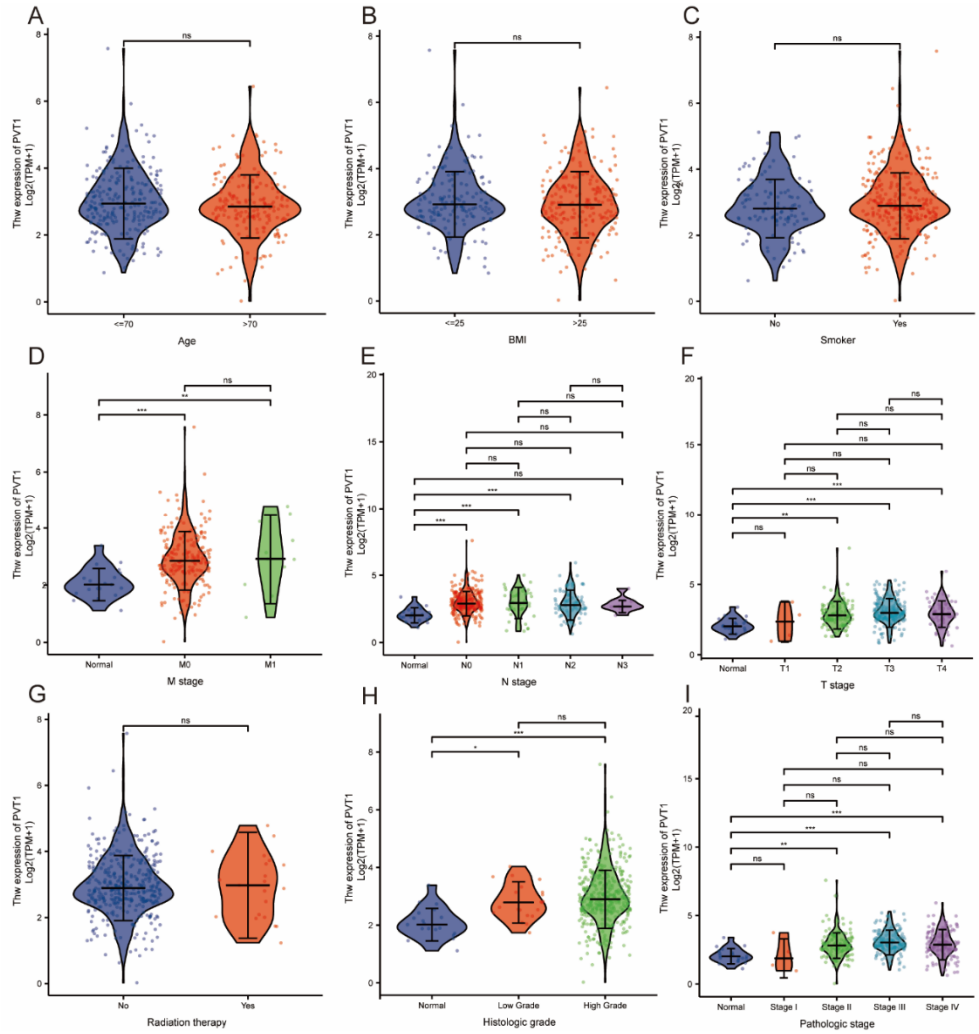

Figure 5. Correlation between PVT1 expression and related clinical indexes, including (A) Age, (B) BMI, (C) smoking status, (D) M stage, (E) N stage, (F) T stage, (G) chemotherapy, (H) histological type, and (I) pathological stage.

Table 2. Baseline data sheet.

Characteristic	Low expression of PVT1	High expression of PVT1	p
n	207	207	
T stage, n (%)			0.196
T1	4 (1.1%)	1 (0.3%)	
T2	66 (17.4%)	53 (13.9%)	
T3	89 (23.4%)	107 (28.2%)	
T4	30 (7.9%)	30 (7.9%)	
N stage, n (%)			0.835
N0	119 (32.2%)	120 (32.4%)	
N1	22 (5.9%)	24 (6.5%)	
N2	41 (11.1%)	36 (9.7%)	
N3	5 (1.4%)	3 (0.8%)	
M stage, n (%)			0.484
M0	105 (49.3%)	97 (45.5%)	
M1	4 (1.9%)	7 (3.3%)	
Pathologic stage, n (%)			0.113
Stage I	3 (0.7%)	1 (0.2%)	
Stage II	73 (17.7%)	57 (13.8%)	
Stage III	61 (14.8%)	81 (19.7%)	
Stage IV	69 (16.7%)	67 (16.3%)	
Radiation therapy, n (%)			1.000
No	182 (46.9%)	185 (47.7%)	
Yes	10 (2.6%)	11 (2.8%)	
Gender, n (%)			0.655
Female	52 (12.6%)	57 (13.8%)	
Male	155 (37.4%)	150 (36.2%)	
Race, n (%)			0.271
Asian	27 (6.8%)	17 (4.3%)	
Black or African American	10 (2.5%)	13 (3.3%)	
White	164 (41.3%)	166 (41.8%)	
Age, n (%)			0.488
<= 70	113 (27.3%)	121 (29.2%)	
> 70	94 (22.7%)	86 (20.8%)	
BMI, n (%)			1.000
<= 25	75 (20.6%)	78 (21.4%)	
> 25	104 (28.6%)	107 (29.4%)	
Histologic grade, n (%)			0.364
High Grade	192 (46.7%)	198 (48.2%)	
Low Grade	13 (3.2%)	8 (1.9%)	
Lymphovascular invasion, n (%)			0.902
No	69 (24.4%)	61 (21.6%)	
Yes	79 (27.9%)	74 (26.1%)	
Smoker, n (%)			0.494
No	59 (14.7%)	50 (12.5%)	
Yes	145 (36.2%)	147 (36.7%)	
Subtype, n (%)			0.326
Non-Papillary	132 (32.3%)	143 (35%)	
Papillary	72 (17.6%)	62 (15.2%)	
Primary therapy outcome, n (%)			0.021
PD	23 (6.4%)	47 (13.2%)	
SD	17 (4.8%)	14 (3.9%)	
PR	12 (3.4%)	10 (2.8%)	
CR	125 (35%)	109 (30.5%)	
Age, meidan (IQR)	69 (60, 75.5)	68 (61, 76.5)	0.917

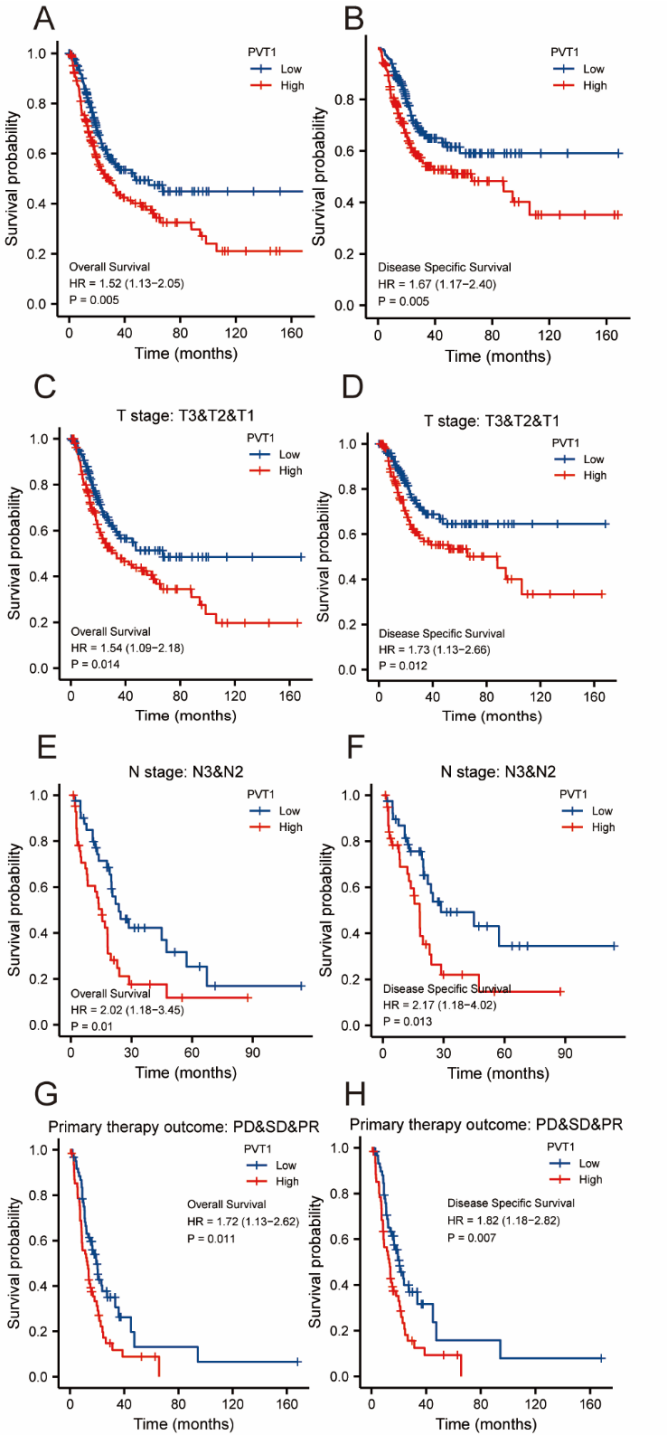

Figure 6. Survival curve evaluating the prognostic value of PVT1. Survival curves using the Kaplan–Meier plotter are shown for OS and DSS. (A,B) Survival curves of OS and DSS in patients with high PVT1 and low PVT1 levels with BLCA. (C,D) OS and DSS survival curves of T1–3 subgroups between PVT1-high and -low patients with BLCA. (E,F) OS and DSS survival curves of N2–3 subgroups between PVT1-high and -low patients with BLCA. (G,H) OS and DSS survival curves of PD&SD&PR subgroups between PVT1-high and -low patients with BLCA. BLCA, bladder urothelial carcinoma; OS, overall survival; DSS, disease specific survival.

Table 3. Univariate regression and multivariate survival methods for prognostic covariates in patients with BLCA (overall survival).

Characteristics	Total(N)	Univariate analysis		Multivariate analysis	
		Hazard ratio (95% CI)	P value	Hazard ratio (95% CI)	P value
T stage (T3&T4 vs. T1&T2)	379	2.199 (1.515–3.193)	**< 0.001**	0.823 (0.165–4.105)	0.813
N stage (N1&N2&N3 vs. N0)	369	2.289 (1.678–3.122)	**< 0.001**	1.097 (0.479–2.511)	0.827
M stage (M1 vs. M0)	213	3.136 (1.503–6.544)	**0.002**	0.945 (0.257–3.471)	0.932
Pathologic stage (Stage III&Stage IV vs. Stage I&Stage II)	411	2.310 (1.596–3.342)	**< 0.001**	2.369 (0.341–16.449)	0.383
Radiation therapy (Yes vs. No)	387	0.965 (0.475–1.964)	0.923		
Primary therapy outcome (CR vs. PD&SD&PR)	357	0.191 (0.136–0.270)	**< 0.001**	0.355 (0.170–0.743)	**0.006**
Gender (Female vs. Male)	413	1.178 (0.855–1.622)	0.316		
Age (> 70 vs. <= 70)	413	1.421 (1.063–1.901)	**0.018**	1.138 (0.586–2.213)	0.702
Race (Asian&Black or African American vs. White)	396	0.873 (0.558–1.368)	0.554		
BMI (> 25 vs. <= 25)	363	0.978 (0.706–1.353)	0.892		
Histologic grade (High Grade vs. Low Grade)	410	2.972 (0.735–12.008)	0.126		
Subtype (Papillary vs. Non-Papillary)	408	0.690 (0.488–0.976)	**0.036**	1.171 (0.529–2.589)	0.697
Lymphovascular invasion (Yes vs. No)	282	2.294 (1.580–3.328)	**< 0.001**	2.065 (0.900–4.735)	0.087
Smoker (Yes vs. No)	400	1.305 (0.922–1.847)	0.133		
PVT1 (High vs. Low)	413	1.525 (1.134–2.050)	**0.005**	2.980 (1.418–6.261)	**0.004**

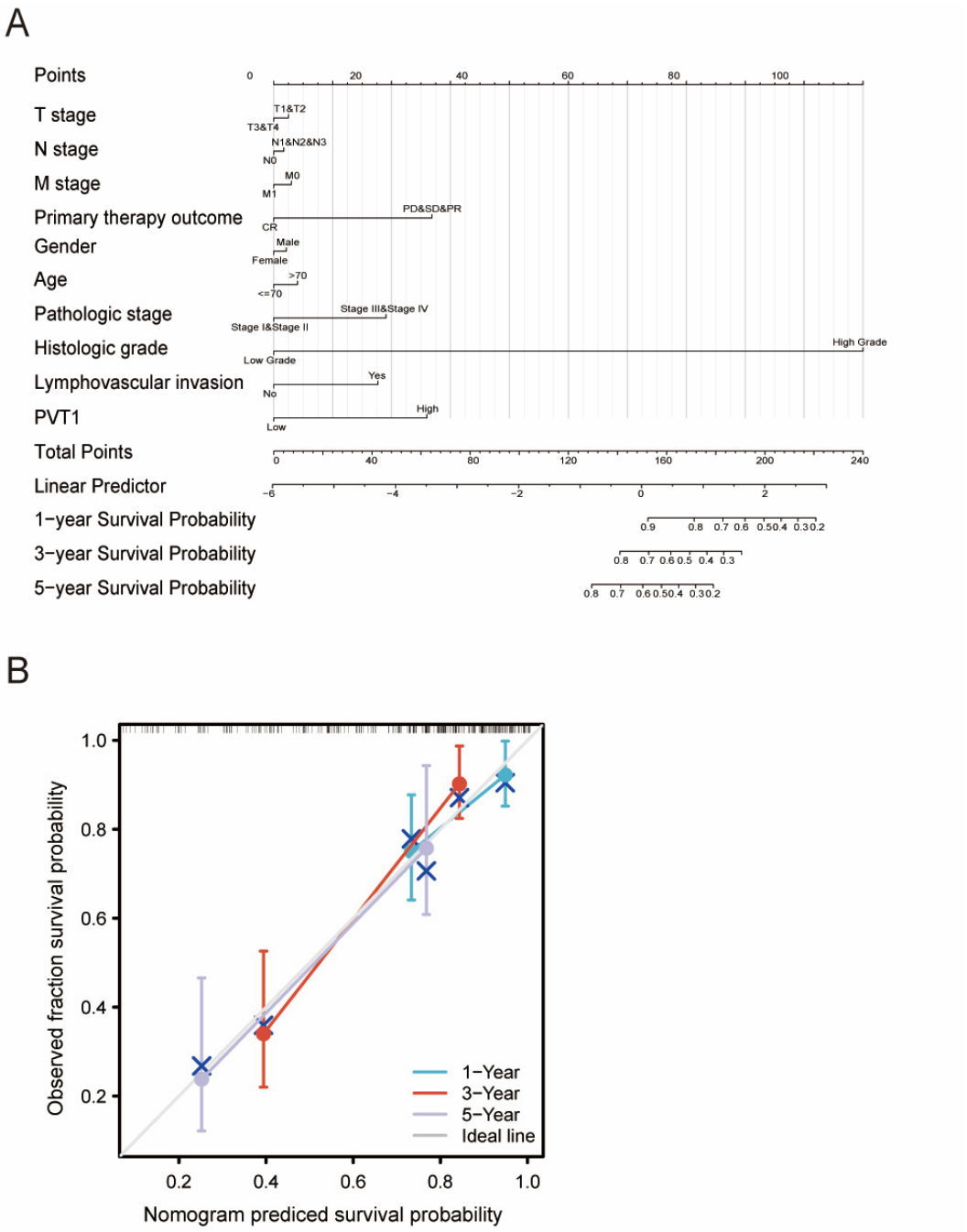

Figure 7. Development and performance of nomogram. Nomogram predicting survival in BLCA patients. (A) The nomogram for predicting the odds of OS at 1, 3 and 5 years in patients with BLCA. (B) Calibration plots comparing predicted and actual overall survival probabilities at 1-, 3- and 5-year follow-up. BLCA, bladder urothelial carcinoma; OS, overall survival.

2.7. Relationship between PVT1 and prognosis of patients with BLCA

The 10-year overall survival (OS) rate of the group with low expression of PVT1 was much higher than that of the group with high expression of PVT1 (HR = 1.52; $P < 0.05$; Figure 6A). Similarly,

the 10-year DSS survival rate in the group with low PVT1 expression was much higher than that in the group with high PVT1 expression (HR = 1.67; $P < 0.05$; Figure 6B).

Univariate Cox regression analysis of clinical indicators showed that T stage (T3&T4 vs. T1&T2) (HR: 2.199; CI: 1.515–3.193; $P < 0.05$), N stage (N1&N2&N3 vs. N0) (HR: 2.289; CI: 1.678–3.122; $P < 0.05$), M stage (M1 vs. M0) (HR: 3.136; CI: 1.503–6.544; $P < 0.05$), pathologic stage (stage III&IV vs. stage I&II) (HR: 2.310; CI: 1.596–3.342; $P < 0.05$), primary therapy outcome (CR vs. PD&SD&PR) (HR: 0.191; CI: 0.136–0.270; $P < 0.05$), age (> 70 vs. <= 70) (HR: 1.421; CI: 1.063–1.901; $P < 0.05$), subtype (papillary vs. non-papillary) (HR: 0.690; CI: 0.488–0.976; $P < 0.05$), and lymphovascular invasion (yes vs. no) (HR: 2.294; CI: 1.580–3.328; $P < 0.05$) were meaningful, and the expression level of PVT1 was also significant (HR: 1.525; CI: 1.134–2.050; $P < 0.05$) (Table 3). After that, we performed subgroup analysis on T stage, N stage, pathologic stage, and primary therapy outcome, and the results are shown in Figures 6C–F.

Multivariate Cox regression was used to screen out independent adverse prognostic factors, and we found that primary therapy outcome (CR vs. PD&SD&PR) and PVT1 (high vs. low) were still meaningful (Table 3).

2.8. Construction and verification of nomogram based on PVT1

To provide a quantitative method for predicting prognosis in patients with uroepithelial carcinoma of the bladder, a nomogram was constructed using PVT1 and independent clinical risk factors (Figure 7A). In the nomogram based on multivariate Cox analysis, points were assigned to these variables using a point scale. The total number of points assigned to each variable was adjusted to a range of 1–100. The points of the variables were accumulated and recorded as total scores. The odds of survival at 1, 3 and 5 years for patients with BLCA was determined by drawing a vertical line directly down from the total point axis to the outcome axis.

The prediction efficiency of the model was analyzed, and the results showed that the C index of the model was 0.748 (CI: 0.706–0.789), indicating that the prediction efficiency of the model was moderate. The deviation correction line in the calibration diagram was close to the ideal curve (45 points), and the predicted values were in good agreement with the observed values (Figure 7B). A nomogram is a better model for predicting short- or long-term survival in patients with gastric cancer.

3. Discussion

To our knowledge, the expression of PVT1 and its potential prognostic impact on BLCA have not been explored. Therefore, the potential role of PVT1 in BLCA is the focus of this study. In this study, bioinformatics analysis was performed using high-throughput RNA sequence data from TCGA database. The results showed that these RNA transcripts had significant individual differences and heterogeneity, and PVT1 might be a potential moderate marker of bladder urothelial carcinoma. High expression of PVT1 in BLCA was associated with higher clinicopathological features, shorter survival, and poorer prognosis.

PVT1 is an active oncogene that plays an important role in the pathogenesis of many tumors [10–15]. PVT1 expression is significantly upregulated in breast cancer tissue compared to that in adjacent normal tissue. The expression of PVT1 is associated with clinical stage, lymph node metastasis, and overall survival of patients with breast cancer [10]. PVT1 is overexpressed in prostate cancer tissues

and cells. The expression of PVT1 is significantly correlated with tumor stage. In addition, PVT1 gene knockout can significantly inhibit the growth of prostate cancer *in vitro* and *in vivo* and promote apoptosis [15]. PVT1 expression was upregulated in 105 human NSCLC tissues compared to normal samples. High PVT1 expression is also associated with a higher TNM stage and tumor size, as well as poorer OS [21].

It has been found that PVT1 has a significant regulatory effect on bladder cancer and can be used as a marker for clinical diagnosis and the treatment of bladder cancer [28]. In this study, we analyzed the expression of PVT1 using the UCSC XENA database, and found that the expression level of PVT1 was altered in a variety of cancers. Subsequently, we used TCGA combined with the GTEx database to select BLCA samples for analysis and confirmed that the expression of PVT1 was increased in cancer patients. We used ROC curve analysis to show that PVT1 had a certain accuracy in the prediction of bladder urothelial carcinoma.

In our study, PVT1 was positively correlated with keratin (KRT) family proteins. The *KRT* gene encodes a set of intermediate filament proteins that form the cytoskeleton of epithelial cells to maintain cell structure under mechanical and non-mechanical cellular stress [30,31]. It has been suggested that in addition to their characteristic mechanical functions, KRTs may play functional roles in apoptosis, cell growth, epithelial polarity, wound healing, and tissue reconstruction [31,32]. In the development of prostate cancer, the presence of a discontinuous KRT5 basal layer is a marker of the transformation process and defines precancerous intraepithelial prostatic neoplasia lesions [33]. KRT13 expression is associated with poor prognosis at multiple stages of disease progression and may be an important biomarker of adverse outcomes in patients with prostate cancer [34]. Keratin (KRT-3/4/13/76/78) is significantly expressed in oral cancers [35]. Increased gene expression of *KRT17*, *KRT14*, and *KRT19* has been detected in the breast cancer cell line WalBC [36]. Some studies have shown that KRT14, KRT5 and KRT20 are associated with bladder cancer subtypes [37,38]. PVT1 is involved in the regulation of a variety of tumors, and our study showed that PVT1 was positively correlated with the expression of the KRT family proteins; however, their relationship in tumors has not yet been investigated and should be studied in the future.

To further investigate the role of PVT1 in BLCA, we performed GO, GSEA, and ssGSEA analyses using TCGA data. A previous study has shown that aberrant methylation of the PVT1 gene is negatively associated with MYC gene expression, and may broadly affect the expression and function of other key genes in two key signaling pathways associated with colorectal cancer: the TGFβ/SMAD and Wnt/β-catenin pathways [8]. Our results showed that the KRAS signaling pathway, P53 signaling pathway, MYC_TARGETS_V1, and other related pathways were enriched to different degrees in the phenotype where PVT1 is highly expressed. It has been reported that the PVT1 promoter inhibits *MYC* expression on the same chromosome through promoter competition, and genome editing has confirmed that PVT1 promoter mutations promote cancer cell growth [39]. *KRAS* has many downstream effector proteins that interact to alter cell survival and proliferation. Active GTP-bound KRAS mainly transmits signals through RAF protein kinase, phosphatidylinositol 3-kinase, guanine nucleotide exchange factor of RAS–associated protein Ral, and phospholipase Cε. RAF initiates a mitogen-activated protein (MAP) kinase cascade that activates extracellular signal-regulated kinase. This active kinase has many targets, including the transcription factor ELK1, which regulates the expression of genes involved in cell cycle progression. The phosphatidylinositol 3-kinase pathway activates Akt, leading to the transcription of survival genes, remodeling of the cytoskeleton, and activation of many transcription factor pathways [40]. A study has shown that *KRAS* carcinogenic mutations drive common metabolic

procedures and promote tumor survival, growth, and immune escape in colorectal cancer, non-small cell lung cancer and pancreatic ductal adenocarcinoma [41].

P53 is one of the most intensively studied tumor suppressors. Mutations or deletions occur in half of all cancers. In the other half, which carry wild-type p53, the p53 signaling pathway is disrupted by abnormalities in other components of the pathway. Due to its important role in tumor inhibition, p53 has attracted great interest in drug development, including gene therapy, activate of p53 by MDM2 and MDMX inhibitors, restore WT p53 activity, mutant p53-based adoptive cell transfer, and other methods [42]. Through GSEA analysis, we found that the differential genes were closely related to the P53 pathway, which will provide a theoretical basis for future studies on the relationship between PVT1 and the P53 pathway.

Our study showed that PVT1 was closely related to Th1, Th2, NKCD56dim cells, and pDCs in immune infiltration. We found that PVT1-related lymphocytes and genes were associated with a subtype of bladder cancer called basal/squamous reported by Kamounetal et al [43]. We speculate that PVT1 might be related to this bladder cancer subtype, which may provide some help for the gene diagnosis and detection of this subtype in the future.

Natural lymphoid cells (ILCs) are present in a variety of tumor types, but their role in tumor immunity is unclear. One study has shown that the immune system plays a key role in the protective response to oral cancer; however, the tumor microenvironment attenuates this anticancer response by regulating the Th response and promoting an anti-inflammatory environment. Regulatory T cells and Th2 effector cells are associated with poor prognosis in oral squamous cell carcinoma [44]. T lymphocytes are a well-studied tumor–infiltrating subgroup. Infiltrated Th cells in tumors are associated with rapid tumor progression [45] and poor prognosis [46]. It has been reported that PVT1 promotes the imbalance of CD4+T cells Th1/Th2 and promotes the hyperproliferation of airway smooth muscle cells [47]. Our study showed that PVT1 was positively correlated with Th1 and Th2 infiltration, and we speculate that PVT1 may create an anti-inflammatory environment and allow tumor cells to survive better by increasing the infiltration of helper T cells.

Unlike traditional T lymphocytes, most ILCs are tissue-resident lymphocytes because they lack antigen-specific receptors. ILCs are involved in immune functions, including pathogen response, inflammation, tissue development, remodeling, repair, and homeostasis. By producing IL-13, ILC2 can recruit dendritic cells (DCs), which drive Th1 and cytotoxic T cell antitumor responses [48]. Our results showed that PVT1 was negatively correlated with the immune infiltration of DCs, which might reduce the infiltration of DCs to avoid the immune response of the tumor. Previous studies have shown that PVT1 expression is positively correlated with CD4+T–cell activation, and PVT1 regulates the proliferation and effector function of CD4+T cells [49]. Our study found that PVT1 was positively correlated with immune infiltration of Th1 and Th2 cells, which is consistent with previous studies. These results suggest that PVT1 may be a potential prognostic marker and therapeutic target for urothelial carcinoma of the bladder.

High expression of PVT1 is associated with poor prognosis. The OS and DSS of patients with high expression of PVT1 were lower than those of patients with low expression of PVT1. In the subgroup analysis of urothelial carcinoma of the bladder, high expression of PVT1 in II-IV, T1-3, N2-3, and PD&SD&PR was associated with poor prognosis. We found that the expression of PVT1 was still a strong predictor of prognosis in these subgroups, indicating that PVT1 was not related to these important clinicopathological parameters. Then, combined with PVT1 and other important clinical types (PVT1 status, TMN stage, main treatment outcome, age status, etc.), a comprehensive evaluation

of the nomogram was carried out. According to the calibration chart, there was good agreement between the actual and predicted values of 1-year, 3-year and 5-year OS. Therefore, our nomogram may be a valuable new prognostic method for clinicians in the future.

Although these results improved our understanding of the relationship between PVT1 and BLCA, there are some limitations. First, to clarify the specific role of PVT1 in the occurrence and development of urothelial carcinoma of the bladder, some clinical parameters need to be considered, such as the details of the patient receiving treatment. However, this information is lacking or inconsistent in public databases. Second, in the current study, there was a large difference between the number of healthy subjects as a control and the number of cancer patients; therefore, additional studies are needed to maintain a balanced sample size. Therefore, a prospective study should be conducted in the future to avoid analytical bias due to the retrospective nature of this study. Finally, since this study was only based on RNA sequencing in TCGA database, it was necessary to further study the direct mechanism of PVT1 in bladder urothelial carcinoma.

4. Materials and methods

4.1. Data source and preprocessing

The paired sample data source UCSC XENA (https://xenabrowser.net/datapages/) using the Toil process [50] unified handling TCGA and GTEx TPM RNAseq data format. BLCA from TCGA and the corresponding normal tissue data from GTEx were extracted. Data translation: transcripts per million reads (TPM) RNA–seq data and log2 transcripts for expression comparison between samples.

Paired sample gene expression data with clinical information from the STAD project (including 19 paracancer tissues and 414 tumor tissues), data was from TCGA (https://portal.gdc.cancer.gov/) BLCA in the project level 3 HTSeq - FPKM RNAseq data format, and RNAseq data were converted from FPKM (Fragments Per Kilobase Per Million) to TPM (transcripts per million reads). Unacquired or unknown clinical features were considered missing values.

4.2. Differential expression of PVT1 in BLCA in TCGA database

Unpaired and paired samples were analyzed using disease status (tumor or normal) as variables to calculate the differential expression of PVT1. The diagnostic accuracy of PVT1 was estimated using an ROC curve. Statistical levels of PVT1 expression above or below the median were defined as PVT1-high or PVT1 low, respectively.

4.3. Analysis of differentially expressed genes (DEGs) in high and low PVT1 expression groups in Bladder Urothelial Carcinoma

Single-gene differences in adjusted P-value < 0.05, $|\text{Log2-fold change}| > 1$. For screening conditions, volcano map visualization was performed for the screened differential genes, and protein-protein interaction (PPI) network analysis was performed using the STRING database and Cytoscape. MCODE was used for PPI network analysis and screening, score > 10 PPI network subsets were selected and PVT1 expression was correlated with heat map analysis.

4.4. Functional enrichment and analysis of immune cell infiltration

PVT1-related differential genes were analyzed using Go and KEGG; R packages, including 'clusterProfiler' (3.14.3 version) (for enrichment analysis) and 'Org.hs.eg. db' (version 3.10.0) (for ID conversion) were used for analysis. Under the condition of p.adj < 0.1 & qvalue < 0.2, there were 123,41 CC, 49 MF and 9 KEGG, while under the condition of p.adj < 0.05 & qvalue < 0.2, there were 68 BP, 10 CC, 33 MF and 9 KEGG.

The differential genes related to PVT1 were analyzed by GSEA, R packet: 'clusterProfiler' package (3.14.3 version) (for GSEA analysis). The reference gene set h.all.v7.2.symbols.gmt (Hallmark). Values of FDR < 0.25 and p.adjust < 0.05, were considered significantly enriched.

The relative tumor infiltration levels of 24 immune cell types were quantified by ssGSEA, GSVA packages are used for analysis [51]. and the immune cells were aDC [activated DC]; B cells; CD8 T cells; Cytotoxic cells; DC; Eosinophils; iDC [immature DC]; Macrophages; Mast cells; Neutrophils; NK CD56bright cells; NK CD56dim cells; NK cells; pDC [Plasmacytoid DC]; T cells; T helper cells; Tcm [T central memory]; Tem [T effector memory]; Tfh [T follicular helper]; Tgd [T gamma delta]; Th1 cells; Th17 cells; Th2 cells [52]. Spearman correlation analysis was used to explore the correlation between PVT1 and the degree of immune cell infiltration and the relationship between immune cell infiltration and different expression groups of PVT1.

4.5. Clinical statistical analysis of prognosis, model construction and evaluation

The R software package (V3.6.3) was used for statistical analysis. The Wilcoxon signed-rank sum test was used to analyze the relationship between PVT1 and clinicopathological features. Patients were grouped according to the expression level of PVT1, and subgroup analysis of overall survival (OS), progression-free interval (PFI) and other clinical characteristics were performed using Cox regression and Kaplan–Meier methods. The effects of PVT1 expression and other clinical features on survival were compared using multivariate Cox analysis. The critical value of PVT1 expression was determined using the median value. Statistical significance was set at $P < 0.05$.

Based on the Cox regression model, the nomogram was established using the independent prognostic factors obtained by multivariate analysis, and the 1-, 3- and 5-year survival probabilities were predicted individually. Data processing was performed using R (version 3.6.3) (Statistical Analysis and Visualization) and R packages 'rms' (version 6.2-0) & survival package (version 3.2-10). By mapping the predicted probability of the nomogram with the observed events, the calibration curve was graphically evaluated, and the 45° line represented the best predicted value. The coordination index was used to determine the degree of discrimination of the nomogram. Supplementary data included prognosis data from a cell article [53].

5. Conclusions

In this study, we report for the first time that the high expression of PVT1 was closely related to the progression, survival, and immune infiltration of BLCA, which may promote tumorigenesis through inflammation and immune response. PVT1 might predict the outcome of treatment and become a new biomarker of BLCA. The mechanism by which PVT1 promotes the progression and metastasis of BLCA should be confirmed in further studies. This study suggests new scope for further

elucidating the clinicopathological significance and molecular mechanisms of bladder urothelial carcinoma.

Authors' contribution

Peiyuan Li played a major role in collecting and analyzing the data, and wrote the manuscript; Gangjie Qiao, Jian Lu and Wenbin Jin performed the visualization operation of correlation analysis; Chao Gao helped to revise the article; Feng Qi designed the experiments and polished the manuscript.

Ethics statement

Ethical review and approval were not required for the study on human participants in accordance with the local legislation and institutional requirements. The patients/participants provided their written informed consent to participate in this study.

Data availability statement

The original contributions presented in the study are included in the article/Supplementary Material. Further inquiries can be directed to the corresponding author.

Conflicts of interest

The authors declare that they have no conflicts of interest.

References

1. L. A. Torre, F. Bray, R. L. Siegel, J. Ferlay, J. Lortet-Tieulent, A. Jemal, Global cancer statistics, 2012, *CA Cancer J. Clin.*, **65** (2015), 87–108. doi: 10.3322/caac.21262.
2. W. J. Kim, S. C. Bae, Molecular biomarkers in urothelial bladder cancer, *Cancer Sci.*, **99** (2008), 646–652. doi: 10.1111/j.1349-7006.2008.00735.x.
3. R. L. Siegel, K. D. Miller, A. Jemal, Cancer statistics, 2016, *CA Cancer J. Clin.*,**66** (2016), 7–30. doi: 10.3322/caac.21332.
4. D. Tolomeo, A. Agostini, G. Visci, D. Traversa, C. T. Storlazzi, PVT1: A long non-coding RNA recurrently involved in neoplasia-associated fusion transcripts, *Gene*, **779** (2021), 145497. doi: 10.1016/j.gene.2021.145497.
5. Y. Y. Tseng, B. S. Moriarity, W. Gong, R. Akiyama, A. Tiwari, H. Kawakami, et al., PVT1 dependence in cancer with MYC copy-number increase, *Nature*, **512** (2014), 82–86. doi: 10.1038/nature13311.
6. Y. Kikuchi, S. Tokita, T. Hirama, V. Kochin, M. Nakatsugawa, T. Shinkawa, et al., CD8+ T-cell immune surveillance against a tumor antigen encoded by the oncogenic long non-coding RNA, PVT1, *Cancer Immunol. Res.*, **9** (2021), 1342–1353. doi: 10.1158/2326-6066.CIR-20-0964.
7. E. Tesfaye, E. Martinez-Terroba, J. Bendor, L. Winkler, C. Olivero, K. Chen, et al., The p53 transcriptional response across tumor types reveals core and senescence-specific signatures modulated by long noncoding RNAs, *Proc. Natl. Acad. Sci. USA*, **118** (2021). doi: 10.1073/pnas.2025539118.

8. K. Shigeyasu, S. Toden, T. Ozawa, T. Matsuyama, T. Nagasaka, T. Ishikawa, et al., The PVT1 lncRNA is a novel epigenetic enhancer of MYC, and a promising risk-stratification biomarker in colorectal cancer, *Mol. Cancer*, **19** (2020), 155. doi: 10.1186/s12943-020-01277-4.
9. Z. Liu, H. Zhang, LncRNA plasmacytoma variant translocation 1 is an oncogene in bladder urothelial carcinoma, *Mol. Cancer*, **8** (2017), 64273–64282. doi: 10.18632/oncotarget.19604.
10. Y. Wang, J. Zhou, Z. Wang, P. Wang, S. Li, Upregulation of SOX2 activated LncRNA PVT1 expression promotes breast cancer cell growth and invasion, *Biochem. Bioph. Res. Commun.*, **493** (2017), 429–436. doi: 10.1016/j.bbrc.2017.09.005.
11. M. Iden, S. Fye, K. Li, T. Chowdhury, R. Ramchandran, J. S. Rader, The lncRNA PVT1 contributes to the cervical cancer phenotype and associates with poor patient prognosis, *PLoS One*, **11** (2016), e0156274. doi: 10.1371/journal.pone.0156274.
12. X. Yu, J. Zhao, Y. He, Long non-coding RNA PVT1 functions as an oncogene in human colon cancer through miR-30d-5p/RUNX2 axis, *J BUON*, **23** (2018), 48–54.
13. Y. R. Yang, S. Z. Zang, C. L. Zhong, Y. X. Li, S. S. Zhao, X. J. Feng, Increased expression of the lncRNA PVT1 promotes tumorigenesis in non-small cell lung cancer, *Int. J. Clin. Exp. Pathol*, **7** (2014), 6929–6935.
14. Y. Wu, W. Gu, X. Han, Z. Jin, LncRNA PVT1 promotes the progression of ovarian cancer by activating TGF-beta pathway via miR-148a-3p/AGO1 axis, *J. Cell Mol. Med.*, (2021). doi: 10.1111/jcmm.16700.
15. J. Yang, C. Li, A. Mudd, X. Gu, LncRNA PVT1 predicts prognosis and regulates tumor growth in prostate cancer, *Biosci. Biotech. Bioch.*, **81** (2017), 2301–2306. doi: 10.1080/09168451.2017.1387048.
16. M. Izadifard, H. Pashaiefar, M. Yaghmaie, M. Montazeri, M. Sadraie, M. Momeny, et al., Expression analysis of PVT1, CCDC26, and CCAT1 long noncoding RNAs in acute myeloid leukemia patients, *Genet. Test. Mol. Bioma.*, **22** (2018), 593–598. doi: 10.1089/gtmb.2018.0143.
17. A. Abbate, D. Tolomeo, I. Cifola, M. Severgnini, A. Turchiano, B. Augello, et al., MYC-containing amplicons in acute myeloid leukemia: genomic structures, evolution, and transcriptional consequences, *Leukemia*, **32** (2018), 2152–2166. doi: 10.1038/s41375-018-0033-0.
18. N. Yazdi, M. Houshmand, A. Atashi, A. Kazemi, A. A. Najmedini, M. N. Zarif, Long noncoding RNA PVT1: potential oncogene in the development of acute lymphoblastic leukemia, *Turk. J. Biol.*, **42** (2018), 405–413. doi: 10.3906/biy-1801-46.
19. H. Handa, K. Honma, T. Oda, N. Kobayashi, Y. Kuroda, K. Kimura-Masuda, et al., Long Noncoding RNA PVT1 Is Regulated by Bromodomain Protein BRD4 in Multiple Myeloma and Is Associated with Disease Progression, *Int. J. Mol. Sci.*, **21** (2020). doi: 10.3390/ijms21197121.
20. A. C. Panda, I. Grammatikakis, K. M. Kim, S. De, J. L. Martindale, R. Munk, et al., Identification of senescence-associated circular RNAs (SAC-RNAs) reveals senescence suppressor CircPVT1, *Nucleic Acids Res.*, **45** (2017), 4021–4035. doi: 10.1093/nar/gkw1201.
21. L. Wan, M. Sun, G. J. Liu, C. C. Wei, E. B. Zhang, R. Kong, et al., Long noncoding RNA PVT1 promotes non-small cell lung cancer cell proliferation through epigenetically regulating lats2 expression, *Mol. Cancer Ther.*, **15** (2016), 1082–1094. doi: 10.1158/1535-7163.MCT-15-0707.
22. C. Zeng, X. Yu, J. Lai, L. Yang, S. Chen, Y. Li, Overexpression of the long non-coding RNA PVT1 is correlated with leukemic cell proliferation in acute promyelocytic leukemia, *J. Hematol. Oncol.*, **8** (2015), 126. doi: 10.1186/s13045-015-0223-4.

23. D. Guo, Y. Wang, K. Ren, X. Han, Knockdown of LncRNA PVT1 inhibits tumorigenesis in non-small-cell lung cancer by regulating miR-497 expression, *Exp. Cell Res.*, **362** (2018), 172–179. doi: 10.1016/j.yexcr.2017.11.014.
24. G. Ping, W. Xiong, L. Zhang, Y. Li, Y. Zhang, Y. Zhao, Silencing long noncoding RNA PVT1 inhibits tumorigenesis and cisplatin resistance of colorectal cancer, *Am. J. Transl. Res.*, **10** (2018), 138–149.
25. X. Z. Wu, H. P. Cui, H. J. Lv, L. Feng, Knockdown of lncRNA PVT1 inhibits retinoblastoma progression by sponging miR-488-3p, *Biomed. Pharmacother.*, **112** (2019), 108627. doi: 10.1016/j.biopha.2019.108627.
26. Y. Cai, J. Wan, Competing endogenous RNA regulations in neurodegenerative disorders: current challenges and emerging insights, *Front. Mol. Neurosci.*, **11** (2018), 370. doi: 10.3389/fnmol.2018.00370.
27. X. Qi, D. H. Zhang, N. Wu, J. H. Xiao, X. Wang, W. Ma, ceRNA in cancer: possible functions and clinical implications, *J. Med. Genet.*, **52** (2015), 710–718. doi: 10.1136/jmedgenet-2015-103334.
28. M. Chen, R. Zhang, L. Lu, J. Du, C. Chen, K. Ding, et al., LncRNA PVT1 accelerates malignant phenotypes of bladder cancer cells by modulating miR-194-5p/BCLAF1 axis as a ceRNA, *Aging (Albany NY)*, **12** (2020), 22291–22312. doi: 10.18632/aging.202203.
29. C. Yu, L. Liu, W. Long, Z. Feng, J. Chen, L. Chao, et al., LncRNA PVT1 regulates VEGFC through inhibiting miR-128 in bladder cancer cells, *J. Cell Physiol.*, **234** (2019), 1346–1353. doi: 10.1002/jcp.26929.
30. V. Karantza, Keratins in health and cancer: more than mere epithelial cell markers, *Oncogene*, **30** (2011), 127–138. doi: 10.1038/onc.2010.456.
31. P. A. Coulombe, M. B. O mary, 'Hard' and 'soft' principles defining the structure, function and regulation of keratin intermediate filaments, *Curr. Opin. Cell Biol.*, **14** (2002), 110–122.
32. R. Moll, M. Divo, L. Langbein, The human keratins: biology and pathology, *Histochem. Cell Biol.*, **129** (2008), 705–733. doi: 10.1007/s00418-008-0435-6.
33. J. I. Epstein, An update of the Gleason grading system, *J. Urol.*, **183** (2010), 433–440. doi: 10.1016/j.juro.2009.10.046.
34. S. Liu, R. M. Cadaneanu, B. Zhang, L. Huo, K. Lai, X. Li, et al., Keratin 13 Is Enriched in Prostate Tubule-Initiating Cells and May Identify Primary Prostate Tumors that Metastasize to the Bone, *PLoS One*, **11** (2016), e0163232. doi: 10.1371/journal.pone.0163232.
35. S. Bundela, A. Sharma, P. S. Bisen, Potential therapeutic targets for oral cancer: ADM, TP53, EGFR, LYN, CTLA4, SKIL, CTGF, CD70, *PLoS One*, **9** (2014), e102610. doi: 10.1371/journal.pone.0102610.
36. J. A. Sharp, S. L. Mailer, P. C. Thomson, C. Lefevre, K. R. Nicholas, Identification and transcript analysis of a novel wallaby (Macropus eugenii) basal-like breast cancer cell line, *Mol. Cancer*, **7** (2008), 1. doi: 10.1186/1476-4598-7-1.
37. L. Lima, M. Neves, M. I. Oliveira, L. Dieguez, R. Freitas, R. Azevedo, et al., Sialyl-Tn identifies muscle-invasive bladder cancer basal and luminal subtypes facing decreased survival, being expressed by circulating tumor cells and metastases, *Urol. Oncol.*, **35** (2017), 675 e1–675 e8. doi: 10.1016/j.urolonc.2017.08.012.

38. M. Eckstein, R. M. Wirtz, M. Gross-Weege, J. Breyer, W. Otto, R. Stoehr, et al., mRNA-expression of KRT5 and KRT20 defines distinct prognostic subgroups of muscle-invasive urothelial bladder cancer correlating with histological variants, *Int. J. Mol. Sci.*, **19** (2018). doi: 10.3390/ijms19113396.
39. S. W. Cho, J. Xu, R. Sun, M. R. Mumbach, A. C. Carter, Y. G. Chen, et al., Promoter of lncRNA Gene PVT1 Is a Tumor-Suppressor DNA Boundary Element, *Cell*, **173** (2018), 1398–1412. doi: 10.1016/j.cell.2018.03.068.
40. Y. Wang, C. E. Kaiser, B. Frett, H. Y. Li, Targeting mutant KRAS for anticancer therapeutics: a review of novel small molecule modulators, *J. Med. Chem.*, **56** (2013), 5219–5230. doi: 10.1021/jm3017706.
41. S. A. Kerk, T. Papagiannakopoulos, Y. M. Shah, C. A. Lyssiotis, Metabolic networks in mutant KRAS-driven tumours: tissue specificities and the microenvironment, *Nat. Rev. Cancer*, **21** (2021), 510–525. doi: 10.1038/s41568-021-00375-9.
42. J. Huang, Current developments of targeting the p53 signaling pathway for cancer treatment, *Pharmacol. Ther.*, **220** (2021), 107720. doi: 10.1016/j.pharmthera.2020.107720.
43. A. Kamoun, A. de Reynies, Y. Allory, G. Sjodahl, A. G. Robertson, R. Seiler, et al., A consensus molecular classification of muscle-invasive bladder cancer, *Eur. Urol.*, **77** (2020), 420–433. doi: 10.1016/j.eururo.2019.09.006.
44. M. Fraga, M. Yanez, M. Sherman, F. Llerena, M. Hernandez, G. Nourdin, et al., Immunomodulation of t helper cells by tumor microenvironment in oral cancer is associated with ccr8 expression and rapid membrane vitamin d signaling pathway, *Front. Immunol.*, **12** (2021), 643298. doi: 10.3389/fimmu.2021.643298.
45. K. D. da Silva, P. C. Caldeira, A. M. Alves, A. C. U. Vasconcelos, A. P. N. Gomes, M. C. F. de Aguiar, et al., High CD3(+) lymphocytes, low CD66b(+) neutrophils, and scarce tumor budding in the invasive front of lip squamous cell carcinomas, *Arch. Oral. Biol.*, **104** (2019), 46–51. doi: 10.1016/j.archoralbio.2019.05.027.
46. O. Stasikowska-Kanicka, M. Wagrowska-Danilewicz, M. Danilewicz, Immunohistochemical analysis of foxp3(+), CD4(+), CD8(+) cell infiltrates and PD-L1 in oral squamous cell carcinoma, *Pathol. Oncol. Res.*, **24** (2018), 497–505. doi: 10.1007/s12253-017-0270-y.
47. Y. Wei, B. Han, W. Dai, S. Guo, C. Zhang, L. Zhao, et al., Exposure to ozone impacted Th1/Th2 imbalance of CD(4+) T cells and apoptosis of ASMCs underlying asthmatic progression by activating lncRNA PVT1-miR-15a-5p/miR-29c-3p signaling, *Aging (Albany NY)*, **12** (2020), 25229–25255. doi: 10.18632/aging.104124.
48. O. Demaria, E. Vivier, Immuno-oncology beyond TILs: Unleashing TILCs, *Cancer Cell*, **37** (2020), 428–430. doi: 10.1016/j.ccell.2020.03.021.
49. J. Fu, H. Shi, B. Wang, T. Zhan, Y. Shao, L. Ye, et al., LncRNA PVT1 links Myc to glycolytic metabolism upon CD4(+) T cell activation and Sjogren's syndrome-like autoimmune response, *J. Autoimmun.*, **107** (2020), 102358. doi: 10.1016/j.jaut.2019.102358.
50. J. Vivian, A. A. Rao, F. A. Nothaft, C. Ketchum, J. Armstrong, A. Novak, et al., Toil enables reproducible, open source, big biomedical data analyses, *Nat. Biotechnol.*, **35** (2017), 314–316. doi: 10.1038/nbt.3772.
51. S. Hanzelmann, R. Castelo, J. Guinney, GSVA: gene set variation analysis for microarray and RNA-seq data, *BMC Bioinformatics*, **14** (2013), 7. doi: 10.1186/1471-2105-14-7.

52. G. Bindea, B. Mlecnik, M. Tosolini, A. Kirilovsky, M. Waldner, A. C. Obenauf, et al., Spatiotemporal dynamics of intratumoral immune cells reveal the immune landscape in human cancer, *Immunity*, **39** (2013), 782–795. doi: 10.1016/j.immuni.2013.10.003.
53. J. Liu, T. Lichtenberg, K. A. Hoadley, L. M. Poisson, A. J. Lazar, A. D. Cherniack, et al., An integrated TCGA pan-cancer clinical data resource to drive high-quality survival outcome analytics, *Cell*, **173** (2018), 400–416. doi: 10.1016/j.cell.2018.02.052.

AIMS Press